論文要旨

Control of Organic Thin Film Growth via Modification of Substrate Surface

(基板表面修飾による有機薄膜の成長制御に関する研究)

金森　由男

Introduction

Organic semiconducting materials have recently attracted considerable attention due to their reduced cost, flexibility, wide applications, and low environmental impact. Over the last few years, performance of organic light emitting diodes (OLEDs) and organic photovoltaic cells (OPVCs) have been greatly improved by designing organic molecules which have appropriate electronic properties. With regard to organic thin film transistors (OTFTs), however, device performance is still far from practical application. What seems to be lacking is crystallinity of thin films rather than

α-sexithiophene

pentacene

Fig. 1 molecular organic semi-conductors studied in this work.

their electronic properties. The subject of this study is to control the morphology of organic thin films by applying appropriate growth condition or novel techniques. We studied organic film growth on electrode metals and insulating dielectrics, via both physical and chemical modification approaches. The target materials are α-sexithiophene (6T) and pentacene, which are depicted in Fig.1.
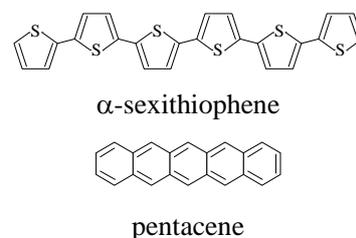
1: Physical modification of dielectric substrate: Graphoepitaxy of a-sexithiophene on periodic grooves

We examined epitaxy on artificially patterned substrates to fabricate high orientated organic thin film. This epitaxy is known as graphoepitaxy and is a promising technique for oriented growth on substrates with an amorphous dielectric top layer. Periodic grooves were fabricated by electron lithography on Si wafers with an oxide layer of 300 nm (Fig.2). The width (W) and depth (d) of the grooves were set at 100 nm and 10 nm, respectively. The periodicity L has various lengths (from 200 nm to 10 µm).

A typical AFM image of 6T films with a thickness of 15 nm is shown in Fig.3. Three different types of 6T grains are observed; facetted grain (FG), elongated facetted grain (EG) and groove filling grain (GFGs). It should be noted that most of GFGs have EGs and FGs on them.

The crystallographic orientation of EGs and FGs can be estimated by their shapes. In-plane orientation of 6T grains can be discussed in terms of θ, which it defined as the angle between b-axis of the 6T grains and the groove direction. The histogram of in-plane orientation of EGs and FGs is depicted in Fig. 4. We can clearly see the following two important

Fig.2 Schematic illustration of a groove pattened substrate. W and d are 100nm and 10nm, respectively.

features; first, there are several peaks in histogram, indicating existence of preferential crystallographic direction. It is likely that these directions are determined to make a low index direction of the grains parallel to grooves (the assignment is shown in Fig.4). We can say that b-direction of 6T films generally tends to be parallel to the grooves for EGs. Second, θ of EGs tends to be small (0 to 45), while that of FGs tends to be large (45 to 90). EGs would be formed as a result of FGs' coalescence on GFGs with small θ. It is worth noting that connection of these EGs is perfect at the coalescence boundary, judging from the extreme flatness of EG surface.
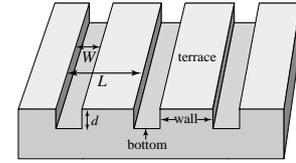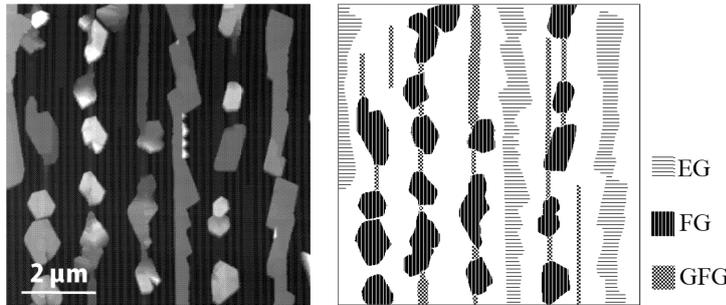
Fig. 3 6T films on periodic groove patterned substrate (L = 200nm).　(Left) An AFM topographic image. (Right) The illustration of classified grains.
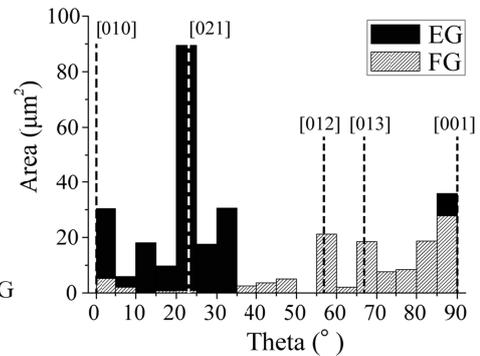
Fig. 4 Histogram showing the distribution of the b-axis direction of 6T grains.

Next, 6T morphology dependence on groove periodicity is examined. At first, densities (n) of three kinds of gains (EGs, FGs and GFGs) are evaluated. The grain density was obtained by calculating the number of grains per unit length normal to the groove, as a function of groove periodicity L. It can be seen in Fig. 5(a) that n$_{GFG}$ decreases gradually obeying a power law in the region of L smaller than 2 µm. It is surprising that $n_{EGandEG}$ remains almost constant, while the site of nucleation decreased with L. This will be attributed to the suppression of nucleation around EGs and FGs. The density of EGs and FGs are determined by the capture length of 6T molecule (Capture zone model). In this model deposited 6T molecules will be immediately captured by the existing island, which results in decrease of the density of 6T migrating molecules and suppression of nucleation around the island. Therefore, nucleation-free regions appeared and the film coverage became small. The capture length L_C can be estimated to be 1 µm. With this model, we can explain why groove periodicity L = 2 µm gives largest EG with this mechanism (see Fig.5(b)). If L is smaller than 2Lc, GFGs would be located at random positions and their capture zones are
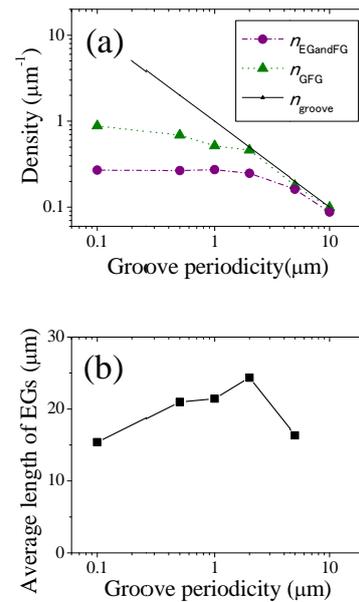
Fig.5 (a) Grain density dependence on groove periodicity.
(b) Average length of EGs at variousove groove periodicity.

overlapped. As a result, each domain could not incorporate sufficient 6T molecules and the elongation is suppressed. When L is larger than $2Lc$, on the other hand, the grain nucleation on terrace occurs and graphoepitaxy is not likely to occur. The optimized L for EGs growth is $L \sim 2L_c, \fallingdotseq 2$ µm.

2: Chemical modification of electrodes: growth of pentacene SAM-modified Au electrodes fabricated on SiO$_2$ substrate

In bottom contact OTFTs, organic semiconductors are deposited on electrodes and dielectric. When the film growth on electrodes is very different from that of on dielectric, the film morphology on dielectric near the electrodes is likely to be influenced by the electrodes. The simplest approach to investigate the electric properties in these regions is to fabricate additional electric probes on the substrates, but this is not applicable since additional electrodes will also influence the film morphology. So we attempted to investigate electric properties without using any additional electrodes by use of frequency response measurement and theoretical analysis we have developed.
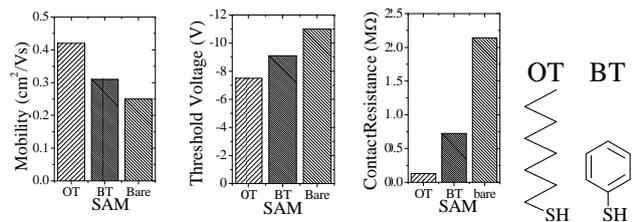
Fig.6 Device performance of SAMs treated pentacene TFTs. Octancethiol and benzenethiol are also depicted.

Two kinds of SAMs, octanethiol (OT : thiol with alkyl chain) and benzenethiol (BT: thiol with aromatic ring), were used in this study. After the fabrication of Au electrodes on SiO$_2$/Si substrates, the substrates were exposed in SAM vapor for 1 day, and then pentacene was deposited in a vacuum chamber. Device performance of fabricated samples is shown in Fig. 6. SAM treated samples showed increase in mobility and decrease in threshold voltage. Contact resistances at electrode-semiconductor interfaces are extracted by analyzing the result of frequency response measurement. Contact resistance dramatically decreases for SAM treated

Fig. 7 (left) The density of off-current carriers. (right) AFM images of organic film disorder near Au electrodes.

samples. Moreover, frequency response measurement also indicates that there are high resistivity and high off current regions near the electrodes. The spatial distribution of off-current carrier is extracted as shown in Fig. 7. Introduction of SAMs could reduce these unexpected regions. Surprisingly, these high-resistivity regions disappear completely in BT-modified samples despite the SAMs effect (on mobility, threshold voltage and contact resistance) seems to be smaller than OT-modified samples. AFM images (Fig.7 right) showed the presence of morphological disorder in a bare sample but not in a BT-modified sample. In these regions electronic states and carrier density are different from those on dielectrics. We have shown that SAMs has the effect to prevent these morphological disorders.
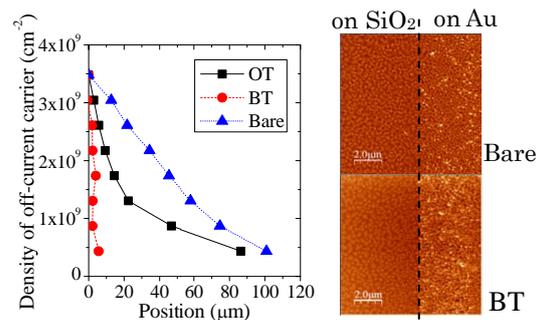
3: A novel dielectric substrate for organic film growth: pentacene growth on graphene oxide

Recently, graphene has attracted much attention due to its unique properties. Graphene oxides (GO), which are obtained as an intermediate substance during chemical fabrication process, are also expected as a novel dielectric of ultrathin thickness. We studied growth of pentacene film on GO substrates for aiming at device application. GO was prepared from natural graphite powder by the Hummer's method. GO flakes were dispersed in methanol. In order to obtain a single or few layers GO film, a highly doped Si substrate

was dipped in the dispersion liquid and lifted. This process yielded GO sheets with various thicknesses on the SiO$_2$/Si substrate. Topographic and current images of GO were measured with SPM measurement system (JEOL JSPM-5200).

First the *I-V* characteristics of GO sheets are measured using conducting cantilever of AFM measurement system. The results are shown in Fig.8. For any GO thickness, electronic conductance is well described by exponential function of $F^{1/2}$, where F is electric field applied normal to the GO sheet. Judging from this kind of field dependence, the conduction mechanism is considered to be Poole-Frenkel emission.

$$I \propto F \exp\left(\frac{\sqrt{q^3 F / 4\pi\varepsilon}}{kT} \right) \quad \text{(eq.1)}$$

Pentacene film deposited onto GO sheets consists of 3D elongated islands and 2D pyramidal layer as shown in Fig. 9(a). From the micro Raman spectroscopy measurement, it is found that orientation of pentacene molecules are lying in elongated islands while pentacene molecules are standing in pyramidal layers. The RHEED images were taken during deposition (Fig.9 (b)). The diffraction pattern is invariant under the in-plane rotation of the sample. Assuming the occurrence of transmission diffraction, the diffraction pattern was simulated. By comparing with experimental data, it is found that pentacene film orientation is likely to have preference of the (021) or (-121) planes parallel to the GO surface. These results showed the crystal structure of 3D elongated islands.
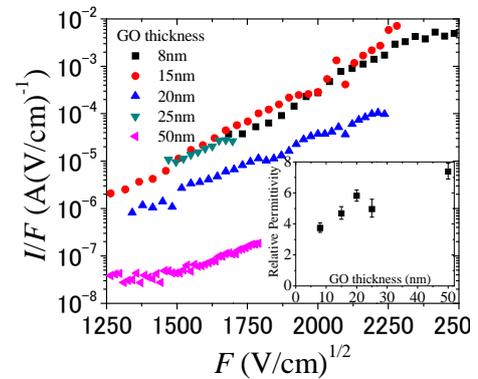

Fig. 8 Poole Frenkel plot for GO sheets. The inset shows relative permittivity calculated by (eq.1).
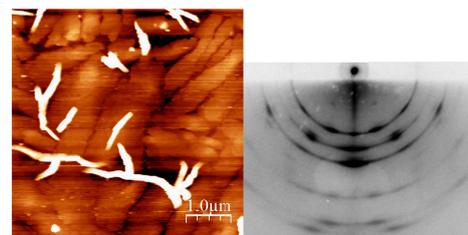

Fig. 9 (left) The AFM image of pentacene of thickness 10 nm deposited on GO sheets. (right) The RHEED image.

Summary

A series of studies about organic film growth on variously modified substrates were conducted in order to control organic molecular orientation. These results solved a part of complexity in OTFTs originating from fragile nature of organic materials. It should be noted that the present results are applicable to other organic molecules and provide fundamental knowledge on the development of organic electronics for practical applications.